OSCILLATIONS IN A BECKER–DÖRING MODEL WITH INJECTION AND DEPLETION *

B. NIETHAMMER†, R.L. PEGO‡, A. SCHLICHTING§, AND J. J. L. VELÁZQUEZ†

Abstract. We study the Becker–Döring bubblelator, a variant of the Becker–Döring coagulation-fragmentation system that models the growth of clusters by gain or loss of monomers. Motivated by models of gas evolution oscillators from physical chemistry, we incorporate injection of monomers and depletion of large clusters. For a wide range of physical rates, the Becker–Döring system itself exhibits a dynamic phase transition as mass density increases past a critical value. We connect the Becker–Döring bubblelator to a transport equation coupled with an integrodifferential equation for the excess monomer density by formal asymptotics in the near-critical regime. For suitable injection/depletion rates, we argue that time-periodic solutions appear via a Hopf bifurcation. Numerics confirm that the generation and removal of large clusters can become desynchronized, leading to temporal oscillations associated with bursts of large-cluster nucleation.

Key words. bubblelator, oscillator, time periodic solution, growth process, injection, depletion, Hopf bifurcation

AMS subject classifications. 68Q25, 68R10, 68U05

1. Introduction.

Becker and Döring [5] provided one of the original descriptions of a mechanism of particle growth in the theory of nucleation from supersaturated vapor. The main assumptions of their model are that individual clusters consist of atomic parts called *monomers*, and that the growth and shrinkage of clusters occurs only by the addition and removal of single monomers. Although this process is not necessarily realized by chemical kinetics, it is convenient to be interpreted as a reaction network of the form

$$\{1\} + \{k\} \underset{b_{k+1}}{\overset{a_k}{\rightleftharpoons}} \{k+1\}\,, \qquad k = 1, 2, 3, \dots\,. \tag{1.1}$$

As noted by Slemrod [34], the Becker-Döring equations provide perhaps the simplest model capable of a realistic description of several phenomena associated with the dynamics of phase changes. Starting from the seminal work of Ball, Carr and Penrose [2], the mathematical theory for these equations has been developed in great detail. Many aspects of the long-time behavior of solutions and the implications for the emergence of phase transitions are understood, but there are also still open questions; see [19] for a recent review.

In this work we add to (1.1) two reaction mechanisms, which are motivated by the dynamics of chemical oscillators, and in particular *bubblelators*, also known as gas evolution oscillators (cf. [35, 8, 39, 4]). First, we suppose monomers are injected into the system at a constant source rate $S > 0$:

$$\emptyset \xrightarrow{S} \{1\}\,. \tag{1.2}$$

*Submitted to the editors March 26, 2022.

Funding: The authors gratefully acknowledge the support of the Hausdorff Research Institute for Mathematics (Bonn), through the Junior Trimester Program on *Kinetic Theory*. This work is supported by the German Research Foundation (DFG) under Germany's Excellence Strategy EXC 2044 – 390685587, *Mathematics Münster: Dynamics–Geometry–Structure* (AS), EXC-2047/1 – 390685813, the *Hausdorff Center for Mathematics*, as well as the Collaborative Research Center 1060 – 211504053, *The Mathematics of Emergent Effects* at the University of Bonn (BN, AS, JV). This material is also based upon work supported by the National Science Foundation under Grant Nos. DMS 1812609 and 2106534 (RLP).

†Institute of Applied Mathematics, University Bonn (niethammer@iam.uni-bonn.de, velazquez@iam.uni-bonn.de).

‡Department of Mathematical Sciences, Carnegie Mellon University (rpego@cmu.edu).

§Applied Mathematics Münster, University Münster (a.schlichting@uni-muenster.de)

Second, we suppose clusters are removed at a rate proportional to a power law with removal coefficient $R > 0$ and exponent $r \geq 0$:

$$\{k\} \xrightarrow{Rk^r} \emptyset, \qquad k = 2, 3, \dots . \tag{1.3}$$

The resulting chemical reaction network (1.1), (1.2), (1.3) is open and no longer satisfies a detailed balance condition, in contrast to (1.1) alone. By consequence, solutions may no longer dissipate free energy, and it becomes unclear whether long-time convergence to equilibrium always holds, or whether some more complicated dynamic behavior becomes possible. In this work we will provide evidence for the persistence of oscillations in time for a suitable approximate model of the network (1.1), (1.2), (1.3).

1.1. The classical Becker–Döring model. The Becker–Döring equations [5] form an infinite system of kinetic equations that describes phase transitions in two-component mixtures where one of the phases has much smaller volume fraction than the other. In this case, the dilute phase consists of clusters of size $k \in \mathbb{N}$, where k denotes the number of atoms, or monomers, in the cluster. The main assumption in the Becker–Döring theory is that clusters evolve only by gain and loss of monomers. If n_k denotes the density of clusters with k monomers, and J_k denotes the net rate of the reaction in (1.1), the equations read

$$\partial_t n_1 = -J_1 - \sum_{k=1}^{\infty} J_k \,, \tag{1.4}$$

$$\partial_t n_k = J_{k-1} - J_k \,, \qquad k \geq 2 \,, \tag{1.5}$$

$$J_k = a_k n_1 n_k - b_{k+1} n_{k+1} \,, \tag{1.6}$$

where a_k, b_k are the respective attachment and detachment rate coefficients. The system of equations (1.4)-(1.6) conserves the total mass ρ; that is,

$$\sum_{k=1}^{\infty} k n_k(t) = \sum_{k=1}^{\infty} k n_k(0) = \rho \,. \tag{1.7}$$

Following work in statistical mechanics done by Penrose and collaborators [28, 29, 30] to model the dynamics of phase transitions, we take the coefficients to be of the form

$$a_k = k^\alpha \,, \qquad b_k = k^\alpha \Big(1 + \frac{q}{k^\gamma}\Big) \,, \qquad \text{with } q > 0 \,,\ \gamma \in (0,1) \,,\ \alpha \in [0,1) \,. \tag{1.8}$$

The exponents α and γ depend upon the geometry of clusters and the dominant mechanism of monomer transport: For three-dimensional spheres dominated by diffusive transport, $\alpha = 1/3$ and $\gamma = 1/3$, while if cluster growth is limited by reactions on the interface, we have $\alpha = 2/3$ and $\gamma = 1/3$. In the two-dimensional situation we have $\gamma = 1/2$ and $\alpha = 0$ and $\alpha = 1/2$, respectively.

The coefficient q arises from the Gibbs-Thomson law and is proportional to surface tension. It plays a key role in determining a critical cluster size k_{crit} during the process of nucleation, a process which will prove fundamental throughout this paper.

We have chosen units for convenience such that the density of monomers in equilibrium with a planar phase boundary is

$$z_s = \lim_{k\to\infty} \frac{b_k}{a_k} = 1.$$

This is also the maximum monomer concentration for which finite-mass steady states exist. The equilibrium state with this critical monomer concentration gives rise to a critical mass $\rho_s > 0$ such that for any $\rho \in [0, \rho_s]$ an equilibrium solution $\bar{n}$ exists, which then has $\bar{n}_1 \le z_s$. For initial data with supercritical mass $\rho > \rho_s$, it has been established in [2, 29] that the solution converges weakly in the long-time limit to the equilibrium solution with density ρ_s. The excess mass $\rho - \rho_s$ is transferred to larger and larger clusters as time proceeds and their evolution can be approximated by the classical LSW model for coarsening (see also [26, 33]). Furthermore, it has been shown in [28] that for certain initial data with small excess density it takes at least exponentially long time (in terms of the excess density) until large clusters are created. Even though the proof is for specific data only, one expects that such metastable behavior appears for all generic data. (See also [11] for numerical simulations.)

1.2. The Becker–Döring model with injection and depletion. In this paper we are interested in the Becker–Döring equations with injection of monomers and depletion of large clusters. More precisely for a given source rate $S > 0$, removal rate $R > 0$ and removal exponent $r \ge 0$, we consider the system

$$\partial_t n_1 = -J_1 - \sum_{k=1}^{\infty} J_k + S\,, \tag{1.9}$$

$$\partial_t n_k = J_{k-1} - J_k - R k^r n_k\,, \qquad k \ge 2\,, \tag{1.10}$$

with J_k as in (1.6) and coefficients as in (1.8).

It is well documented in the chemistry literature that temporal oscillations can persist in chemical–physical systems in which a phase transition creates strong nucleation peaks that lead to rapid growth of supercritical agglomerations which are later removed. Specifically, the system (1.9)–(1.10) has many similarities to models of bubblelator dynamics describing oscillatory release of a gas (cf. [25, 1, 35, 31, 17]). For more background, we refer to Section 1.7.

Our goal is to obtain oscillatory solutions for an approximation of the model (1.9)-(1.10) under suitable choices of the source term S and the removal term R. The rough heuristics explaining the appearance of oscillatory solutions are the following. For small S and R, the solution of (1.9), (1.10) first evolves as in the classical model without source and removal terms—indeed, it evolves to a metastable steady state with locally constant nonzero fluxes J_k. Slowly, the source term S kicks in and raises the monomer density to a supercritical value with a small positive excess $n_1 - 1 > 0$ of order ε for small $\varepsilon > 0$. This triggers the creation (or nucleation) of clusters larger than a critical size. The nucleated supercritical clusters then grow by a process that depletes the monomer density by a smaller amount of order $\varepsilon^{1/\gamma}$ which is nevertheless enough to shut down large-cluster creation. Large clusters eventually get destroyed, nucleation resumes, and the scenario repeats.

In order for this picture to be realized, the source term S and the removal term R have to be chosen in such a way that all the relevant terms balance. At steady state, source-driven nucleation balances removal of very large clusters. But the time it takes for nucleated clusters to grow large enough for effective removal introduces a delay that allows creation and removal to get out of phase.

1.3. Limit model. In Section 2 we identify the relevant scales, determine suitable S and R and derive a simplified model formally valid in the limit $\varepsilon \to 0$. This consists of an evolution equation for a rescaled monomer density u, defined in terms of the excess monomer density via

$$n_1 - 1 = \varepsilon + \left(\frac{\varepsilon}{q}\right)^{1/\gamma} u\,, \tag{1.11}$$

and a transport equation for a rescaled density f of large clusters with rescaled continuous size $x \in (0,\infty)$. Section 2.5 contains the precise definition of the scales and a rescaled removal rate $\eta > 0$. Taking those for granted, we formally derive the system

$$\partial_\tau u(\tau) = 1 - \int_0^\infty x^\alpha f(x,t), dx\,, \tag{1.12}$$

$$\partial_\tau f(x,\tau) + \partial_x\big(x^\alpha f(x,\tau)\big) = -\eta x^r f(x,\tau)\,, \qquad x > 0\,, \tag{1.13}$$

$$x^\alpha f(x,\tau) \to e^{u(\tau)}\,, \qquad x \to 0\,. \tag{1.14}$$

The key ingredients that go into the derivation of this system are the following. First, the distribution of clusters for k around the critical size $k_{\rm crit}$ or smaller is taken as quasistationary, corresponding to constant-flux states for the Becker-Döring equations, which are parametrized by the monomer density. The transport equation arises by a continuum approximation to the difference equation (1.5) in the supercritical range $x \simeq (k - k_{\rm crit})/X > 0$, with size scale X exponentially large in ε. The two size regimes are related by matching fluxes around $k \simeq k_{\rm crit}$. For the quasistationary states, a continuum approximation results in an Arrhenius law giving the exponential dependence on u in (1.14). The precise scaling of u by $\varepsilon^{1/\gamma}$ leads to a change of order one in the Arrhenius factor in the boundary condition (1.14) when u has a change of order one.

We remark that a simple computation yields the mass balance law

$$\partial_\tau \left(u(\tau) + \int_0^\infty x f(x,\tau)\, dx \right) = 1 - \eta \int_0^\infty x^{r+1} f(x,\tau)\, dx. \tag{1.15}$$

Hence, the total mass in the system increases though the influx of monomers in (1.12) at unit rate, and decreases due to the removal of large clusters on the right hand side of (1.13).

1.4. Oscillations via Hopf bifurcation. For the approximate model (1.12)–(1.14), time-periodic solutions satisfy a delay-differential equation with infinite delay horizon. To our knowledge, a mathematically rigorous Hopf bifurcation theorem has been proven only for finite delay horizons. Nevertheless, we argue in Section 3 that Hopf bifurcations from stationary solutions should occur as one varies the removal parameter η. In particular, we make a careful analysis of the spectrum of the linearized problem around a steady state solution and track the dependence of the eigenvalues of the linearized operator upon the removal parameter η. We identify points where eigenvalues cross the imaginary axis transversely, and we perform a formal expansion to determine the direction that bifurcation should occur, which should indicate when *stable* periodic solutions appear. We provide analytical and numerical evidence regarding bifurcation points and their dependence on α and r in Section 4.

1.5. Oscillations via desycronization of source and removal. In Figure 1 a numerical solution of the limit model (1.12)–(1.14) is shown. The oscillations are large amplitude, indicating that the chosen parameters are already far beyond the Hopf bifurcation point. The flux profiles in this regime develop an interesting structure involving the transport of rather sharp peaks, which one can understand in a physical way that we wish to explain.

Before discussing that, we remark that stable oscillations should also exist in the full Becker–Döring model with injection and depletion (1.9), (1.10). The numerical computation of such oscillations seems to be a challenging matter, however, due to the multiscale nature of the Becker–Döring system, as already observed in [11]. The main difficulty is that the scales associated to the problem depend exponentially on the small parameter ε. For instance, we obtain for $\varepsilon = 0.1$ that the typical

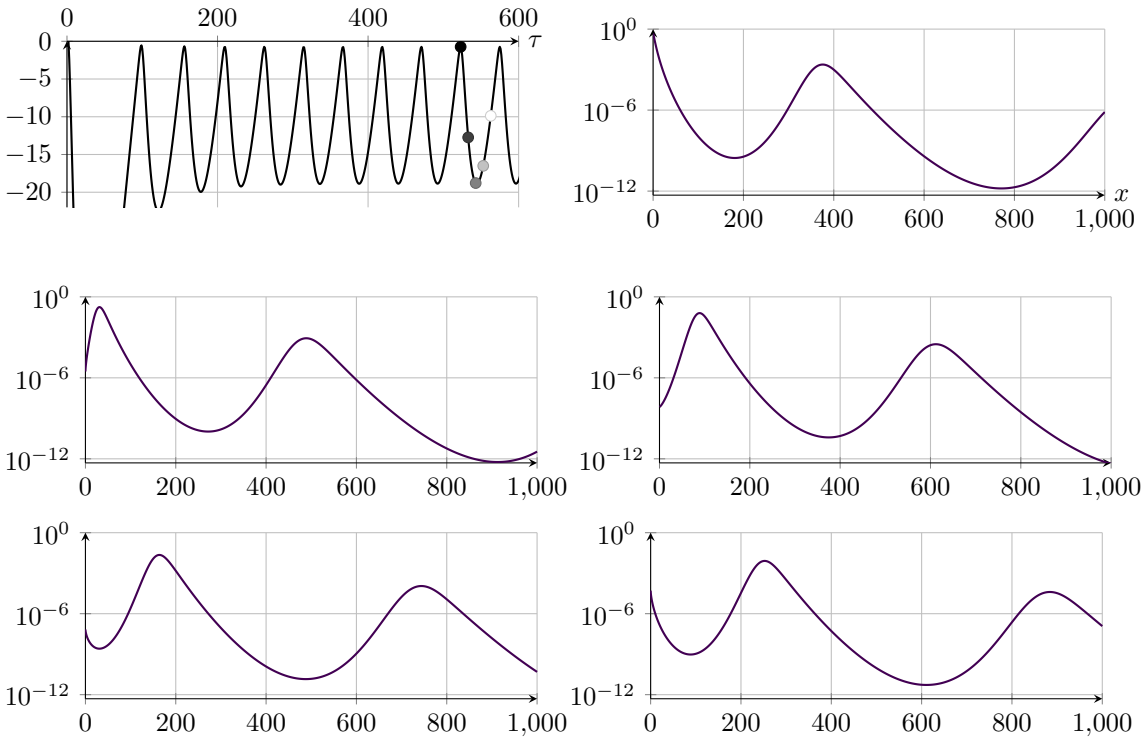

Fig. 1: Time evolution of u (top left), and semi-log plots of flux $x^\alpha f$ at times $\tau = 523$ (top right), $\tau = 533$ and 543 (middle row), $\tau = 553$ and 563 (bottom row). The times $\tau = 523, \dots, 563$ are indicated by circle marks in the top left plot. Parameters: $\eta = 0.1$, $\alpha = \frac{1}{3}$, $\gamma = \frac{1}{3}$, $r = \frac{2}{3}$.

size of clusters that are involved in the dynamics of the system (1.9), (1.10) is of order 10^{12} with a typical time-scale of order 10^9 (cf. Subsection 2.5). For larger values of ε a numerical approach might be feasible, but the formal asymptotic approximation done in this paper may not apply.

In Figure 2, different fluxes in the Becker–Döring model relevant for the description of the oscillation mechanism are shown, superimposed on a schematic and highly exaggerated plot of n_k *vs* k. The first crucial quantity is the *critical size* k_{crit}, as in [28]. This depends on the monomer excess $\varepsilon = n_1 - 1$, and is defined for simplicitiy here as the value of k for which $a_k n_1 - b_k$ vanishes (cf. Section 2.1). For the rates (1.8) and recalling that $z_s = 1$, it holds

$$k_{\text{crit}} = \left(\frac{q}{\varepsilon}\right)^{\frac{1}{\gamma}}. \tag{1.16}$$

In the following, the critical size k_{crit} is used to distinguish small from supercritical clusters. It also provides the relevant next scale for the monomer expansion in (1.11), since $n_1 - 1 = \varepsilon + u/k_{\text{crit}}$. The first driving mechanism is the flux of mass through the small clusters to beyond the critical size k_{crit}, denoted by J_{nuc}. In the literature (cf. Friedlander [17]), this process is called *homogeneous nucleation*. Because this process is diffusion-dominated for k around k_{crit}, we obtain a boundary layer with size of order $\varepsilon^{-1/\gamma}$, resulting in an Arrhenius relation for the flux. This is reflected in the

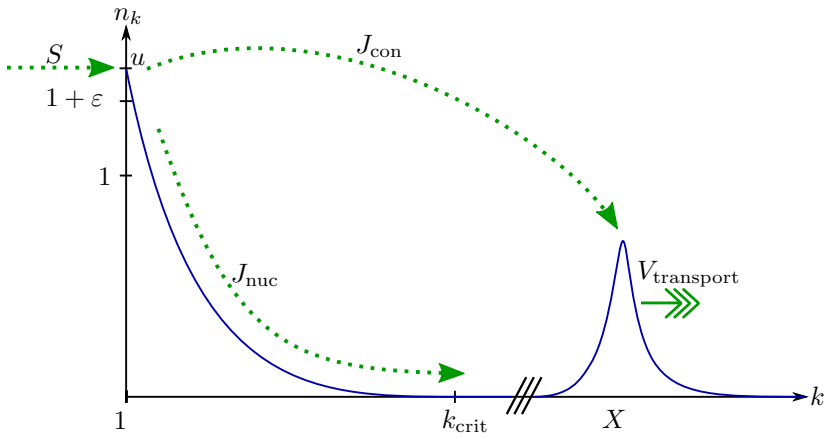

Fig. 2: Illustration of transport mechanisms (not to scale). For explanation, see text.

limit model through the exponential boundary condition (1.14).

A second flux $J_{\rm con}$ depletes the monomer concentration through the mechanism of large-cluster growth by direct absorption of monomers, also called *condensation*. This flux is reflected in the limit model as the integral loss term in (1.12), and also leads to the transport term in (1.13).

These two fluxes need to be balanced with the source term S, and the time-scale chosen accordingly, which is done in a careful analysis of the scales in Section 2.5.

Both systems, the Becker–Döring model (1.9)–(1.10) and the limit model (1.12)–(1.14), allow for stationary states with time-independent concentration of monomers, and we believe that these are stable for large depletion parameters R or η, respectively. However, our results indicate that time-periodic solutions of the limit model exist for small particle-removal rates.

An explanation is that in this case clusters must grow very large for effective removal. This depletes the monomer concentration due to the condensation flux $J_{\rm con}$ that drives the growth of large clusters, and leads to time delays in replenishing those clusters. It takes more time both to restart nucleation from a lower monomer level and to grow supercritical clusters to sizes large enough for removal. In this way the generation and removal of large clusters can *desynchronize*, resulting in temporal oscillations.

In somewhat more detail, the mechanism for oscillations works as follows. Peaks in the size distribution of large clusters form through a process mediated by the sensitive (exponential) dependence of the nucleation rate upon the concentration of monomers: A sufficient excess of monomers above the critical concentration $n_1 = 1$ triggers rapid growth of the number of supercritical clusters through nucleation. The creation of enough supercritical clusters then produces a large condensation flux $J_{\rm con}$ which forces the concentration of monomers to decrease in spite of the source term. This stops, or drastically slows, the nucleation reaction transferring mass through the critical size.

The peak of supercritical clusters generated in this way then continues to be transported to ever-larger sizes by the condensation mechanism, which continues to consume monomers. At sufficiently large sizes, the rate that clusters are removed from the system becomes dominant and the peak is eliminated. This makes the condensation flux $J_{\rm con}$ small again, which allows the source term to

force the monomer concentration higher, and start the cycle over.

1.6. Sharp peak model. The mechanism for oscillations just described can be implemented in a simple model with only two elements, namely the excess monomer density $u(t)$ and the size distribution $f(x,t)$ for clusters of supercritical size $x > x_{\rm crit}$. The clusters increase their size at some constant rate by absorbing monomers, and they are removed instantaneously when size reaches some terminal value $x_{\rm rm} > x_{\rm crit}$. If the source of monomers drives their excess to reach a certain nucleation threshold $u_{\rm nuc}$, a sudden *sharp peak* of large clusters is created just above the critical size.

The balance law for the monomer excess takes the form

$$\partial_t u(t) = 1 - \int_{x_{\rm crit}}^{x_{\rm rm}} f(x,t)\,dx, \tag{1.17}$$

and one starts with initial excess $u(0) < u_{\rm nuc}$ below the nucleation threshold. The size distribution f is advected at constant speed 1, satisfying the transport equation

$$\partial_t f + \partial_x f = 0, \qquad x_{\rm crit} < x < x_{\rm rm}. \tag{1.18}$$

We specify a zero influx condition $f(x_{\rm crit},t) = 0$ as long as the monomer flux remains below threshold, i.e., $u(t) < u_{\rm nuc}$. When the monomer excess reaches the threshold at some time t_*, however, a delta-mass concentration of supercritical clusters is instantly nucleated at $x = x_{\rm crit}$, giving the jump condition

$$f(\cdot,t_*^+) = f(\cdot,t_*^-) + f_0\delta_{x_{\rm crit}} \qquad \text{if} \quad u(t_*) = u_{\rm nuc}. \tag{1.19}$$

For $f_0 > 1$ and $f \equiv 0$ initially, say, this model produces a sawtooth evolution for u, with $\partial_t u = 1 > 0$ during time intervals when no supercritical clusters exist in the system, and $\partial_t u = 1 - f_0 < 0$ during intervals after a peak of clusters has been nucleated and before it is removed upon reaching the outflow boundary $x = x_{\rm rm}$.

The resulting oscillatory evolution in this model clearly illustrates desynchronization of supercritical cluster generation and removal. The first two equations (1.17) and (1.18) of this model are very similar to (1.12) and (1.13) by setting $\alpha = 0$ and letting $r \to \infty$. The only main difference is that the exponential boundary condition (1.14) is changed to the jump condition (1.19), leading here to the periodic production of sharp peaks.

1.7. Related literature. Oscillations in chemical reaction networks have been well known ever since the Belousov–Zhabotinsky reaction was described [6, 40] and the *Brusselator* found by Prigogine and Lefever [32] (see [37] for the name). Later, the *Oregonator* was introduced by Field and Noyes [16] as a simpler model that develops temporal oscillations involving only five species. The mathematical analysis of these systems reveals that the basic mechanism behind the oscillations is of Lotka–Volterra type [21, 22, 38].

In contrast to this, the model from Section 1.2 is motivated by mechanisms found in the dynamics of *bubblelators*, also known as gas evolution oscillators [35, 8, 39, 4]. These are chemical–physical systems [36] in which, due to some reaction mechanism, a dissolved gas is constantly generated in a solvent, leading to a steady increase in supersaturation and an eventual burst of nucleation and growth of gas bubbles. The first experimental report of such a system is ascribed to Morgan [25], who observed an oscillatory release of gas during dehydration of formic acid in concentrated sulfuric acid. The dynamics and growth of bubbles resembles a mechanism similar to

the Becker–Döring paradigm: The growth of bubbles is effected mainly through the absorption of gas emerging from the supersaturated solution into the expanding bubbles. Upon discretization in size, this suggests that the physical growth mechanism is reflected by fluxes resembling those in (1.6). Lastly, large bubbles randomly leave the solvent, depending on the setup of the experiment, mainly due to buoyancy, and this is loosely reflected in the system (1.10) by the removal term $-Rkrn_k$.

More experimental evidence of oscillatory concentrations in a mixture of nitric oxide and coal gas was obtained by Badger and Dryden [1]. A theoretical model of Becker–Döring type was proposed by Pratsinis, Friedlander, and Pearlstein [31] (cf. also [17]). The model in [31] has some physical similarities with the limit model obtained in Section 1.3. More precisely, the model uses the exponent $\alpha = 2/3$ in (1.8) and $r = 0$ in (1.10). In this case, it is possible to obtain a closed system of ODEs for the evolution of the three lowest-order moments of the distribution of radii of supercritical clusters. This system of ODEs is coupled with the concentration of monomers n_1 by means of an Arrhenius formula yielding the nucleation rate of supercritical clusters as a function of the monomer concentrations. The resulting model in [31] is a system of ODEs for which the existence of periodic solutions is demonstrated using a Hopf bifurcation argument. A similar reduction of a Becker–Döring model to a system of ODEs which has periodic solutions can be found in [24]. We can show (see the Appendix A) that, for some particular choices of exponents, the limit model from Section 1.3 can be reduced to a system of ODEs which has the same structure as those obtained in [17, p. 293ff].

A boundary condition similar to (1.14) was derived by Farjoun and Neu [14] in a physical study describing the depletion of a supercritical concentration of monomers (without source) due to the nucleation of supercritical clusters. The nucleation rate is approximated using an Arrhenius law (or Frank-Kamanetskii) type of formula. A key observation made in [14] in the derivation of this boundary condition is that small changes in the concentration of monomers n_1 yield significant changes in the nucleation rate. This same point underpins the present study.

Recently, oscillations for a Becker–Döring model with atomization were proved to exist by two of the present authors in [27]. The model in [27] is closed and has no external source or removal terms ($S = r = 0$ in (1.9)–(1.10)). The atomization of clusters of a maximal size M into M monomers provides a closed feedback mechanism from large clusters to monomers, which could be considered to replace injection and depletion. This model has a Hopf bifurcation for suitable small atomization rate, when M is large.

In the physical literature, temporal oscillations in coagulation-fragmentation models permitting interactions of clusters of any sizes (thus not of Becker-Döring type) have been reported in numerical simulations, by R. C. Ball et al. [3] for cases with monomer injection and cluster removal above a fixed size, and in the works [23, 9] for cases incorporating a nonlinear atomization mechanism. The onset of a Hopf bifurcation for a model consisting of coagulation with monomers and atomization has been recently shown numerically in [10].

Lastly, Doumic et al. [13] consider a model for prion dynamics of Becker–Döring type, which exhibits very slowly damped oscillations. The model in [13] assumes that the polymer chains interact with two types of chemicals yielding respectively increase and decrease of the length of the polymer chain. These chemicals interact between themselves by means of a modified Lotka–Volterra type of equation, which is coupled with the Becker–Döring part of the system. It is well known that Lotka–Volterra models may admit periodic solutions. The interaction of the Lotka–Volterra equation with the Becker–Döring part is responsible for the damping of the oscillations observed in [13], but the specific form in which this damping takes place is not well understood at the moment.

2. Derivation of the limit model. In this section, we describe a regime in which the discrete Becker–Döring model with source and depletion (1.9)–(1.10) can be formally approximated by the limit model (1.12)–(1.14).

Our analysis is based on understanding the interaction between small and large clusters, where the separation scale is given by the critical size (1.16). We shall argue that for clusters smaller or comparable to $k_{\rm crit}$, solutions are close to a constant-flux steady state of the Becker–Döring equation parametrized by the monomer concentration, and we derive an Arrhenius law relating the flux and monomer concentration. We provide additional discussion of the quasistationary assumption in the supplementary material SM1, where we describe the time scale for a drift-diffusion approximation in the boundary layer where k is near critical size.

In Section 2.2, we show that the dynamics of large clusters are well approximated by a transport equation, which will rescale to (1.13). The boundary condition for this transport equation is obtained in Section 2.3 by matching with the fluxes from Section 2.1. Then in Section 2.4, we study the evolution of the monomer fluctuation u in (1.11). This is a balance between (i) the nucleation flux towards large clusters through the critical size $k_{\rm crit}$ and (ii) a condensation flux due to the growth of large clusters.

Finally, in Section 2.5, we will identify a time scale T, a macroscopic cluster size scale X much larger the critical cluster size (1.16), a macroscopic cluster density F, as well as the source rate S and the depletion rate R for which the Becker–Döring system (1.9)–(1.10) with injection and depletion can be approximated by the limit model (1.12)–(1.14).

2.1. Steady states with constant flux. We recall results from [28] about steady states with constant flux. We consider in particular the case of small excess density and find suitable asymptotic expressions of the steady states in this regime. It is convenient to recall first the formulas for equilibrium solutions with zero flux, given by

$$\bar n_k = Q_k \bar n_1^k\,, \qquad Q_k = \prod_{l=1}^{k-1} \frac{a_l}{b_{l+1}}\,, \tag{2.1}$$

where the parameter $\bar n_1$ represents the equilibrium concentration of monomers. With coefficients as in (1.8) we find

$$\log(a_k Q_k) = \log\left(\prod_{l=1}^{k} \frac{a_l}{b_l}\right) = \sum_{l=1}^{k} \log\left(\frac{1}{1+\frac{q}{l^\gamma}}\right) \simeq -\frac{q k^{1-\gamma}}{1-\gamma}(1+o(1)) \qquad \text{as } k\to\infty. \tag{2.2}$$

Thus we see that the series $\sum_{k=1}^\infty k Q_k \bar n_1^k$, which represents the mass of $(\bar n_k)$, has radius of convergence 1 and converges for $\bar n_1 = 1$. The corresponding critical mass is denoted as $\rho_s = \sum_{k=1}^\infty k Q_k$.

For super-critical monomer density $\bar n_1 > 1$, the zero-flux equilibrium solution $Q_k \bar n_1^k$ grows exponentially at infinity and those solutions will not play a role. As in [28] we consider in this regime steady states with constant flux, where the flux is chosen such that the steady state remains bounded as $k\to\infty$. More precisely, we look for given $\bar n_1$ for bounded solutions $\{N_k(\bar n_1)\}_{k=\mathbb{N}}$ of

$$N_1 = \bar n_1 \qquad \text{and} \qquad a_{k-1}\bar n_1 N_{k-1}(\bar n_1) - b_k N_k(\bar n_1) = J(\bar n_1)\,, \qquad k\ge 2\,, \tag{2.3}$$

where $J(\bar n_1)$ is part of the unknown. It has been shown in [28, Lemma 1] that for each $\bar n_1 > 1$ there exists a unique solution to this problem, given by the formula

$$N_k(\bar n_1) = J(\bar n_1) Q_k \bar n_1^k \sum_{l=k}^\infty \frac{1}{a_l Q_l \bar n_1^{l+1}} \qquad \text{where} \qquad \frac{1}{J(\bar n_1)} = \sum_{l=1}^\infty \frac{1}{a_l Q_l \bar n_1^{l+1}}\,. \tag{2.4}$$

Furthermore, for fixed $\bar{n}_1$, $a_k N_k(\bar{n}_1)$ decreases monotonically with k (which implies that $N_k(\bar{n}_1)$ is bounded and $N_k(\bar{n}_1) \to 0$ as $k \to \infty$ if $\alpha > 0$), while for fixed k, $\frac{N_k(\bar{n}_1)}{\bar{n}_1}$ increases monotonically with $\bar{n}_1$ and we have for $\bar{n}_1 > 1$ that $Q_k < N_k(\bar{n}_1) < Q_k \bar{n}_1^k$ for $k \in \mathbb{N}$.

Asymptotics of steady states and flux. We are particularly interested in the asymptotic behavior of $\{N_k(\bar{n}_1)\}_{k=\mathbb{N}}$ and $J(\bar{n}_1)$ for slightly supercritical density $\bar{n}_1 > 1$. Thus we introduce the small parameter

$$\varepsilon = \bar{n}_1 - 1 \ll 1\,. \tag{2.5}$$

We shall argue that the asymptotics for the constant flux are given by

$$J(\bar{n}_1) \simeq J_\infty := \sqrt{\frac{\gamma}{2\pi q^{\frac{1}{\gamma}}}} \varepsilon^{\frac{\gamma+1}{2\gamma}} \exp\left(-\frac{\gamma}{1-\gamma} q^{\frac{1}{\gamma}} \varepsilon^{-\frac{1-\gamma}{\gamma}}\right) \qquad \text{as } \varepsilon \to 0, \tag{2.6}$$

and for the corresponding steady states by

$$N_k(\bar{n}_1) \simeq \frac{J(\bar{n}_1)}{\varepsilon a_k} = \frac{J(\bar{n}_1)}{\varepsilon k^\alpha} \qquad \text{for } k \gg k_{\text{crit}} = \left(\frac{q}{\varepsilon}\right)^{\frac{1}{\gamma}}. \tag{2.7}$$

Derivation of (2.6). The critical cluster size k_{crit} from (1.16) is a crucial quantity occurring in the analysis of this paper, as in [28]. Improving on (2.2), we can write

$$\frac{1}{a_k Q_k \bar{n}_1^k} = e^{G(k)}(1 + o(1))\,, \qquad \text{with} \quad G(k) = -k \log \bar{n}_1 + \int_1^k \log(1 + q l^{-\gamma})\, dl + C\,. \tag{2.8}$$

The series for $1/J(\bar{n}_1)$ in (2.4) is dominated by terms with l near the point where $k \mapsto G(k)$ is maximized, and it happens exactly at $k_{\text{crit}} = (q/\varepsilon)^{1/\gamma}$, which is consistent with (1.16). Laplace's method provides an approximation to the series: Noting that

$$G''(k) = \frac{-\gamma q k^{-\gamma-1}}{1 + q k^{-\gamma}}$$

and $G'''(k)/G''(k) = O(1/k)$, the expansion $G(k) = G(k_{\text{crit}}) + \frac{1}{2} G''(k_{\text{crit}})(k - k_{\text{crit}})^2 (1 + o(1))$ is valid for $|k - k_{\text{crit}}| < k_{\text{crit}}^p$ for any $p < 1$. Choosing $p > \frac{1}{2}(1 + \gamma)$ allows $k_{\text{crit}}^{-\gamma-1}(k - k_{\text{crit}})^2$ to be large, whence we find

$$\sum_{|l - k_{\text{crit}}| < k_{\text{crit}}^p} \frac{1}{a_l Q_l \bar{n}_1^l} \simeq e^{G(k_{\text{crit}})} \int_{-\infty}^{\infty} e^{\frac{1}{2} G''(k_{\text{crit}})(k - k_{\text{crit}})^2}\, dk = e^{G(k_{\text{crit}})} \sqrt{\frac{2\pi}{-G''(k_{\text{crit}})}} \qquad \text{as } \varepsilon \to 0. \tag{2.9}$$

The remaining part of the series for $1/J(\bar{n}_1)$ is small relative to this, and since $n_1 \simeq 1$ it follows (2.6) from $J(\bar{n}_1) \simeq \sqrt{\frac{-G''(k_{\text{crit}})}{2\pi}} e^{-G(k_{\text{crit}})}$ and by noting that

$$G(k_{\text{crit}}) \simeq \frac{q k_{\text{crit}}^{1-\gamma}}{1-\gamma}(1 + o(1)) - k_{\text{crit}} \log \bar{n}_1 \simeq \frac{k_{\text{crit}} \varepsilon \gamma}{1-\gamma} = \frac{\gamma}{1-\gamma} q^{\frac{1}{\gamma}} \varepsilon^{1 - \frac{1}{\gamma}}. \tag{2.9}$$

Derivation of (2.7). Similarly we obtain by recalling the relation (2.8) for $k \gg k_{\text{crit}}$ that

$$a_k Q_k \bar{n}_1^k \sum_{l=k}^{\infty} \frac{1}{a_l Q_l \bar{n}_1^l} \simeq e^{-G(k)} \sum_{l=k}^{\infty} e^{G(l)} \simeq \int_0^{\infty} e^{G'(k) l}\, dl = \frac{1}{-G'(k)} \simeq \frac{1}{\varepsilon}\,,$$

and hence, from (2.4), we obtain (2.7).

2.2. Transport equation for large clusters. For clusters much larger than the critical size, exceeding the macroscopic cluster size scale X that will be determined below in Section 2.5, we have

$$J_k = a_k\big(n_1{-}1\big)n_k - \frac{a_k q}{k^\gamma}n_k + b_k n_k - b_{k+1}n_{k+1} \simeq a_k \varepsilon n_k \quad \text{for } k \gg X \gg k_{\rm crit}\,. \tag{2.10}$$

Hence, we can approximate the evolution of clusters in this regime by

$$\partial_t n(k,t) + \varepsilon \partial_k\big(k^\alpha n(k,t)\big) = -rk^r n(k,t) \tag{2.11}$$

where for large cluster sizes, we treat k a continuous variable and we represent the discrete concentration $n_k(t)$ by a continuous concentration $n(k,t)$.

2.3. Monomers and the nucleation flux. The behavior of n for clusters that are much larger than the critical size, but much smaller than X, is given by the quasistationary solutions depending on $n_1(t)$, that is (2.7) implies

$$k^\alpha n(k,t) \simeq \frac{J(n_1(t))}{\varepsilon} \qquad \text{for } k_{\rm crit} \ll k \ll X\,. \tag{2.12}$$

We see from (2.6) that small changes in ε yield large changes in the flux $J(1+\varepsilon)$. In order to obtain variations of order one during the evolution we introduce a rescaled concentration of monomers. More precisely, we introduce for fixed $0 < \varepsilon \ll 1$ the new variable u via

$$n_1(t) = 1 + \varepsilon + \left(\frac{\varepsilon}{q}\right)^{\frac{1}{\gamma}} u(t) = \bar n_1 + \frac{u(t)}{k_{\rm crit}}\,.$$

Note also that we have $n_1{-}1 \simeq \varepsilon$ at leading order as long as $u = O(1)$. Hence, as long as u remains of smaller order, we may approximate $J(n_1)$ with n_1 in place of $\bar n_1$ in the derivation of (2.6) to arrive at

$$J(n_1) \simeq J_\infty e^u\,. \tag{2.13}$$

Indeed, the relation (2.13) follows by maximizing

$$\tilde G(k) = -k\log n_1 + \int_1^k \log(1+ql^{-\gamma})\,dl + C = G(k) - k\log\left(\frac{n_1}{\bar n_1}\right).$$

The maximum occurs at $\tilde k$ satisfying $n_1 = 1 + q\tilde k^{-\gamma}$, so

$$\tilde k = \left(\frac{q}{n_1-1}\right)^{\frac{1}{\gamma}} = \left(\frac{q}{\varepsilon}\right)^{\frac{1}{\gamma}}\left(\frac{n_1-1}{\varepsilon}\right)^{-\frac{1}{\gamma}} = k_{\rm crit}\left(1+\frac{u}{\varepsilon k_{\rm crit}}\right)^{-\frac{1}{\gamma}} = k_{\rm crit} + O(\varepsilon^{-1}).$$

Hence, by following the same derivation as for (2.6), we arrive at $J(n_1) \simeq J(\bar n_1)e^{-\tilde G(\tilde k)+G(k_{\rm crit})}$. Now $\tilde k = k_{\rm crit}(1+o(1))$, so

$$\tilde k \log\left(\frac{n_1}{\bar n_1}\right) = \tilde k \log\left(1+\frac{u}{k_{\rm crit}\bar n_1}\right) = u + o(1)\,,$$

while $G(\tilde k) - G(k_{\rm crit}) = O(G''(k_{\rm crit})(\tilde k - k_{\rm crit})^2) = O(k_{\rm crit}^{-1-\gamma}\varepsilon^{-2}) = O(\varepsilon^{\frac{1}{\gamma}-1})$ justifying the asymptotic expansion (2.13).

2.4. Evolution of monomers. We introduce a constant $L \gg 1$ as a multiplicative cutoff between subcritical and supercritical clusters, and approximate the equation for the monomers by

$$\partial_t n_1 = -J_1 - \sum_{k=1}^{Lk_{\rm crit}} J_k - \sum_{k=Lk_{\rm crit}+1}^{\infty} J_k + S\,.$$

In the second sum we use the approximation (2.10) for the fluxes J_k and approximate the sum by an integral

$$\sum_{k=Lk_{\rm crit}+1}^{\infty} J_k \simeq (n_1-1)\int_{Lk_{\rm crit}+1}^{\infty} n(k,t)k^\alpha\,dk \qquad \text{for } L \gg 1.$$

In the supplementary material SM1, we justify that in the region of of subcritical clusters, the evolution follows a quasistationary law on an algebraically large time scale in ε^{-1}, which allows us to approximate J_k by $J(n_1(t))$ for $1 \le k \le Lk_{\rm crit}$.

Using also that $n_1 - 1$ is of order ε we obtain the following equation for the concentration of monomers

$$\frac{1}{k_{\rm crit}}\partial_t u = -\big(Lk_{\rm crit}+1\big)J(n_1(t)) - \varepsilon\int_{Lk_{\rm crit}+1}^{\infty} f(y,t)y^\alpha dy + S\,, \tag{2.14}$$

together with equation (2.11) for the supercritical clusters and the boundary condition (2.12). We will see later that the term $(Lk_{\rm crit}+1)J$ in the contribution of the monomers is negligible compared to the integral term during the whole dynamics. We assume that for the moment and will check that *a posteriori*.

2.5. Identification of scales. We introduce new units and variables for the cluster size X, x time T, τ and cluster density F, f, respectively, via

$$k = Xx\,, \qquad t = T\tau\,, \qquad n = Ff\,. \tag{2.15}$$

We will obtain the limit model (1.12)–(1.14) by choosing the scales

$$X = \left(\frac{\varepsilon}{k_{\rm crit}J_\infty}\right)^{\frac{1}{2-\alpha}}, \quad T = \frac{X^{1-\alpha}}{\varepsilon}, \quad F = \frac{k_{\rm crit}}{X^2}, \quad S = \frac{1}{Tk_{\rm crit}}, \quad R = \frac{\eta}{TXr}, \tag{2.16}$$

with $k_{\rm crit}$ as defined in (1.16) and J_∞ given in (2.6). We have also included the size of the monomer source S in this formula and introduce a rescaled depletion rate $\eta > 0$. Notice that from (2.6), J_∞ is exponentially small in the parameter ε, which implies similar exponential dependencies for all scales X, T, F, and S.

Using the scales in (2.15), the monomer equation (2.14) becomes

$$\partial_\tau u = -\big(Lk_{\rm crit}+1\big)J(n_1(\tau))Tk_{\rm crit} - \varepsilon X^{1+\alpha}FTk_{\rm crit}\int_{\frac{Lk_{\rm crit}+1}{X}}^{\infty} f(x,\tau)x^\alpha dx + STk_{\rm crit}\,, \tag{2.17}$$

and similarly the transport equation for the large clusters (2.11) together with its boundary conditions (2.12) take the form

$$\partial_\tau f(x,\tau) + \frac{T\varepsilon}{X^{1-\alpha}}\partial_x\big(x^\alpha f(x,\tau)\big) = -\big(TX^rR\big)x^r f(x,\tau) \tag{2.18}$$

$$x^\alpha f(x,\tau) \simeq \frac{J(n_1(\tau))}{F\varepsilon X^\alpha}, \qquad \text{for } \frac{k_{\rm crit}}{X} \ll x \ll 1\,. \tag{2.19}$$

We recall from (2.13) that $J(n_1(\tau)) = J_\infty e^{u(\tau)}$, where J_∞ is an exponentially small quantity defined in (2.6) that gives the order of magnitude of the fluxes through the critical size. As explained in Section 1.5, the nucleation rate, given by the flux through the critical size manifested as the boundary condition in (2.19), and the condensation rate, given by the coagulation rate of monomers with macroscopic clusters manifested as the scale of the integral in (2.17), need to be of the same order of magnitude. It is readily checked that (2.16) implies

$$\frac{J_\infty}{F\varepsilon X^\alpha} = 1 \qquad \text{and} \qquad \varepsilon X^{1+\alpha} F T k_{\rm crit} = 1\,.$$

The time scale that yields growth of the macroscopic clusters due to the transport on the left hand side of (2.18) in that scale is given by $T\varepsilon/X^{1-\alpha}$, which becomes equal to one by the choice (2.16).

Notice that the choice of S in (2.16) implies that the changes of u in (2.17) are of order one. This justifies the expansion of the flux in (2.13) *a posteriori* This formula yields the relation between ε and the source S. A different choice of S might still result in oscillatory behavior, with an amplitude change in u not of order $O(1)$, although the expansion of the flux in (2.13) is valid for u up to order $o(\varepsilon^{-\frac{1}{\gamma}})$.

In order to conclude the derivation of the limit model (1.12)–(1.14), it only remains to justify neglecting the fluxes in the subcritical region, or equivalently to show that the term $(Lk_{\rm crit} + 1)J(n_1(\tau))Tk_{\rm crit}$ in (2.17) is negligible. The contribution $Lk_{\rm crit} + 1$ is algebraically large in ε^{-1}. We estimate the exponential terms contained in the product $J(n_1(\tau))T$, which are

$$J_\infty \Big(\frac{1}{J_\infty}\Big)^{\frac{1-\alpha}{2-\alpha}} = J_\infty^{1-\frac{1-\alpha}{2-\alpha}} = J_\infty^{\frac{1}{2-\alpha}}\,. \tag{2.20}$$

Since $\frac{1}{2-\alpha} > 0$, it follows that this term is exponentially small. Therefore the flux terms due to subcritical particles yield a negligible contribution and (2.17) can be formally approximated by (1.12).

3. Periodic solutions for the limit problem. Our goal is to argue, by formal means, that steady state solutions of the limit model (1.12)–(1.14) undergo a Hopf bifurcation as the rescaled removal parameter η is varied, for a wide range of values of α and r.

To our knowledge, a rigorous Hopf bifurcation theorem has not yet been proven for a model of this type, though it seems plausible that one might extend existing methods for retarded functional differential equations with finite delays (RFDE) which are based upon rescaling to fix the temporal period and Lyapunov-Schmidt reduction [18, 12].

It is well known, that in order to prove the existence of periodic solution by means of a Hopf bifurcation, one has to show:

1. existence of steady states for a family of dynamical systems parametrized by $\theta \in \Theta$;
2. the linear stability of these steady states changes at a critical value $\theta_{\rm crit}$ due to fact that two complex conjugated eigenvalues of the linearized system cross from $\{\mathrm{Re}(\lambda) < 0\}$ to $\{\mathrm{Re}(\lambda) > 0\}$;
3. for generic dynamic systems, the periodic solutions exists for small $|\theta - \theta_{\rm crit}|$ either in the parameter region $\{\theta < \theta_{\rm crit}\}$ or $\{\theta > \theta_{\rm crit}\}$. These periodic solutions are stable if the steady states found in 1. are unstable for the range of θ, where the periodic solutions exist.

We carry out the three steps of this program for the limit model (1.12)–(1.14) in Subsections 3.1, 3.2, 3.3, respectively. To simplify the Hopf bifurcation analysis, it is convenient to introduce a new size variable z and relabeled flux $h(z,\tau)$ defined by

$$z = x^{1-\alpha} \qquad \text{and} \qquad h(z,\tau) = \frac{x^\alpha g(x,\tau)}{1-\alpha}\,, \tag{3.1}$$

In those variables the system (1.12)–(1.14) takes the form

$$\partial_\tau u = 1 - \int_0^\infty h(z,\tau) z^\nu \, dz\,, \tag{3.2}$$

$$\partial_\tau h(z,\tau) + \partial_z h(z,\tau) = -\eta z^\beta h(z,\tau)\,, \qquad z>0\,, \tag{3.3}$$

$$h(0,\tau) = e^{u(\tau)}\,, \tag{3.4}$$

where the exponents β and ν are nonnegative and given by

$$\beta = \frac{r}{1-\alpha}\,, \qquad \nu = \frac{\alpha}{1-\alpha}\,. \tag{3.5}$$

For any solution of this system, such as a steady-state or time-periodic solution, which exists for all times $\tau \in \mathbb{R}$, one finds, by integrating (3.3) along characteristics emerging from $z=0$, that necessarily

$$h(z,\tau) = \exp(u(\tau - z)) \exp\Big(-\frac{\eta}{\beta+1} z^{\beta+1}\Big)\,. \tag{3.6}$$

Using this expression in (3.2) we find that u must satisfy an RFDE with infinite delay, namely

$$\partial_\tau u = 1 - \int_0^\infty e^{u(\tau-z)} \exp\Big(-\frac{\eta}{\beta+1} z^{\beta+1}\Big) z^\nu dz\,. \tag{3.7}$$

3.1. Steady states and their stability. For any $\eta > 0$ we have a constant solution $u \equiv u_0$ of this equation, given by

$$1 = e^{u_0} \int_0^\infty \exp\Big(-\frac{\eta}{\beta+1} z^{\beta+1}\Big) z^\nu dz\,. \tag{3.8}$$

The corresponding steady state $h = h_0(z)$ is then given by (3.6) with u replaced by u_0.

Next we consider the linear stability of these steady states as solutions of (3.2)–(3.4). After linearizing about u_0, h_0, we find nonzero solutions proportional to $e^{\lambda\tau}$ exist, $\lambda \in \mathbb{C}$, if and only if

$$\lambda = -e^{u_0} \int_0^\infty \exp\Big(-\frac{\eta}{\beta+1} z^{\beta+1} - \lambda z\Big) z^\nu dz\,. \tag{3.9}$$

It is convenient to study this equation after the rescaling $\eta^{-\frac{1}{\beta+1}}\lambda \mapsto \lambda$. With

$$G_{\beta,\nu}(\lambda) := \int_0^\infty \exp\Big(-\frac{1}{\beta+1} z^{\beta+1} - \lambda z\Big) z^\nu dz\,, \tag{3.10}$$

the eigenvalue equation (3.9) then takes the form

$$\vartheta\lambda + G_{\beta,\nu}(\lambda) = 0, \qquad \text{where} \quad \vartheta = \eta^{\frac{1}{\beta+1}} G_{\beta,\nu}(0)\,. \tag{3.11}$$

Note $\lambda = 0$ is never an eigenvalue since $G_{\beta,\nu}(0) > 0$. Also note $G'_{\beta,\nu}(\lambda) = -G_{\beta,\nu+1}(\lambda)$,

$$G_{\beta,\nu}(0) \geq |G_{\beta,\nu}(\lambda)| \quad \text{and} \quad |G'_{\beta,\nu}(0)| \geq |G'_{\beta,\nu}(\lambda)| \quad \text{whenever } \operatorname{Re}\lambda \geq 0. \tag{3.12}$$

It follows that we have linear stability for large values of the parameter ϑ:

LEMMA. *There are no eigenvalues in the closed right half plane if $\vartheta > |G'_{\beta,\nu}(0)|$, i.e.,*

$$\eta > \left(\frac{G_{\beta,\nu+1}(0)}{G_{\beta,\nu}(0)}\right)^{\beta+1}.$$

The reason is that if $\operatorname{Re}\lambda \geq 0$, then with $G = G_{\beta,\nu}$ we have

$$\vartheta > |G'(0)| \geq \operatorname{Re}\left(\frac{G(0) - G(\lambda)}{\lambda}\right) \geq -\operatorname{Re}\frac{G(\lambda)}{\lambda}.$$

3.2. Eigenvalue crossings. A Hopf bifurcation should occur provided that some branch of solutions $\lambda = \lambda(\vartheta)$ of (3.11) crosses the imaginary axis transversely. This means that $\operatorname{Re}\lambda = 0$ and $\operatorname{Re}\frac{d\lambda}{d\vartheta} \neq 0$ at some particular $\vartheta = \vartheta_0$. Since $(\vartheta + G'(\lambda))\frac{d\lambda}{d\vartheta} = -\lambda$ along the branch, we find

$$\operatorname{sign}\operatorname{Re}\frac{d\lambda}{d\vartheta} = \operatorname{sign}\operatorname{Re}\Big(-\lambda\big(\vartheta + \overline{G'(\lambda)}\big)\Big) = \operatorname{sign}\frac{d}{dt}\operatorname{Re}G(it) = \operatorname{sign}\frac{d}{dt}\arg G(it), \tag{3.13}$$

if $\lambda = it$ with $t > 0$. Thus the criteria for Hopf bifurcation become the following: First, there should exist $t_0 > 0$ such that for $t = t_0$,

$$\operatorname{Re}G_{\beta,\nu}(it) = 0 \quad \text{and} \quad \operatorname{Im}G_{\beta,\nu}(it) < 0, \quad \text{or equivalently} \quad \arg G_{\beta,\nu}(it) = -\frac{\pi}{2} \pmod{2\pi}. \tag{3.14}$$

This is necessary and sufficient for (3.11) to hold with $\vartheta = -G(it)/it > 0$. Second, the transversality condition holds if and only if

$$\frac{d}{dt}\operatorname{Re}G_{\beta,\nu}(it) \neq 0, \qquad \text{or equivalently} \qquad \frac{d}{dt}\arg G_{\beta,\nu}(it) \neq 0. \tag{3.15}$$

Thus we can provide evidence that a Hopf bifurcation occurs (for some ϑ) and infer the direction of eigenvalue crossings by identifying zero crossings on the graph of $\frac{\pi}{2} + \arg G(it) \pmod{2\pi}$. In the original time scale τ of the model, such zeros correspond to oscillations with wave number

$$\kappa = t\eta^{\frac{1}{\beta+1}} = \frac{t\vartheta}{G_{\beta,\nu}(0)}, \qquad G_{\beta,\nu}(0) = (\beta+1)^{\frac{\nu-\beta}{\beta+1}}\Gamma\left(\frac{\nu+1}{\beta+1}\right). \tag{3.16}$$

3.3. Direction of bifurcation. In this section we identify computable criteria that should determine the direction of bifurcation (i.e., whether small time-periodic solutions appear for $\eta > \eta_0$ or $\eta < \eta_0$). We posit bifurcating solutions have variable period $2\pi/\kappa$ and scale time using the variable wave number κ near a value κ_0 given by (3.16) at a putative bifurcation point $t = t_0$. Rewriting (3.7) in terms of the constant solution u_0 from (3.8) and rescaled variables given by

$$u(\tau) = u_0 + U(s), \qquad s = \kappa\tau, \qquad y = \kappa z, \tag{3.17}$$

we find that the 2π-periodic function U, constant κ and bifurcation parameter η should satisfy

$$\kappa\partial_s U + \int_0^\infty \left(e^{U(s-y)} - 1\right)\exp\left(\frac{-\eta}{\beta+1}\frac{y^{\beta+1}}{\kappa^{\beta+1}}\right) y^\nu\, dy \frac{e^{u_0}}{\kappa^{\nu+1}} = 0. \tag{3.18}$$

It will be convenient to work with the variables and parameters given by

$$v(s) = e^{U(s)} - 1, \qquad \delta = \frac{\kappa^{\nu+2}}{e^{u_0}}, \qquad \mu = \frac{\eta}{(\beta+1)\kappa^{\beta+1}}, \qquad g(\mu, y) = y^\nu \exp(-\mu y^{\beta+1}). \tag{3.19}$$

Thus we seek a 2π-periodic function v, constant δ and bifurcation parameter μ so

$$\delta \partial_s v + (1+v)(\gamma * v) = 0, \qquad \text{where} \quad (\gamma * v)(s) = \int_0^\infty g(\mu, y) v(s-y)\, dy. \tag{3.20}$$

The function $v \equiv 0$ is a trivial solution for any δ and μ, and the problem is equivariant with respect to translation in s. We expect bifurcation from this branch for δ, μ respectively near values δ_0, μ_0 coming from the parameters t_0, η_0 by the formulas above.

In terms of an amplitude parameter ε, we seek formal expansions

$$v = \varepsilon v_1 + \varepsilon^2 v_2 + \dots, \quad \delta = \delta_0 + \varepsilon \delta_1 + \varepsilon^2 \delta_2 + \dots, \quad \mu = \mu_0 + \varepsilon \mu_1 + \varepsilon^2 \mu_2 + \dots.$$

We will find $\delta_1 = \mu_1 = 0$ as is typical for Hopf bifurcation. Provided certain nondegeneracy conditions hold, we find the quantities δ_2 and μ_2 can be expressed in terms of the quantities

$$\hat{g}_j(k) = \int_0^\infty e^{-iky} g_j(y)\, dy, \qquad g_j(y) = \partial_\mu^j g(\mu_0, y) = (-y^{\beta+1})^j y^\nu \exp(-\mu_0 y^{\beta+1}). \tag{3.21}$$

In fact, our computations will show that μ_2 and δ_2 are determined by the relations

$$\mu_2 \operatorname{Re} \hat{g}_1(1) = \frac{-\delta_0^2 \operatorname{Re} \hat{g}_0(2)}{4|\hat{g}_0(2) + 2i\delta_0|^2}, \qquad \delta_2 + \mu_2 \operatorname{Im} \hat{g}_1(1) = -\frac{\delta_0}{4} + \frac{\delta_0^2 (2\delta_0 + \operatorname{Im} \hat{g}_0(2))}{4|\hat{g}_0(2) + 2i\delta_0|^2}, \tag{3.22}$$

provided the transversal crossing condition and the nonresonance condition $\hat{g}_0(2) + 2i\delta_0 \neq 0$ hold.

Returning to the original parameters $\eta = \eta_0(1 + \varepsilon^2 \eta_2 + \dots)$, $\kappa = \kappa_0(1 + \varepsilon^2 \kappa_2 + \dots)$, and taking from (3.8) into account that $e^{u_0} G_{\beta,\nu}(0) = \eta^{\frac{\nu+1}{\beta+1}}$, we find

$$\eta_2 = (\nu+2)\frac{\mu_2}{\mu_0} + (\beta+1)\frac{\delta_2}{\delta_0}, \qquad \kappa_2 = \frac{\nu+1}{\beta+1}\frac{\mu_2}{\mu_0} + \frac{\delta_2}{\delta_0}. \tag{3.23}$$

The sign of η_2 determines the direction of the bifurcation. It is plausible that this determines the stability of the bifurcating periodic solutions in a similar way as for ODEs, and RFDEs with finite delays [12]. Namely, if the constant flux solution with $u \equiv u_0$ is stable for η on one side of the bifurcation point η_0, then bifurcating periodic solutions are stable if they appear for η on the opposite side, and unstable otherwise. As the constant-flux solution is stable for η sufficient large, we therefore expect that *at the largest bifurcation point η_0, the new branch of periodic solutions is stable provided that η_2 is negative.* We call this case *supercritical* and will provide numerical evidence that indeed such bifurcations occur in Section 4.2.

In the remainder of this section we derive the relations in (3.22). By an integration by parts starting from (3.13), we have $\lambda = it = -\bar{\lambda}$, since $\frac{d}{dy} e^{-ity} = -ite^{-ity}$. Moreover, $G'_{\beta,\nu}(\lambda) = -G_{\beta,\nu+1}(\lambda)$ and hence by using (3.11), we obtain

$$-\bar{\lambda} G'_{\beta,\nu}(\lambda) = -itG_{\beta,\nu+1}(it) = \int_0^\infty \left(\frac{d}{dy} e^{-ity}\right) y^{\nu+1} \exp\Big(-\frac{y^{\beta+1}}{\beta+1}\Big) dy$$

$$= -\int_0^\infty e^{-ity}((\nu+1)y^\nu - y^{\nu+1+\beta})\exp\Big(-\frac{y^{\beta+1}}{\beta+1}\Big)dy$$

$$= -(\nu+1)G_{\beta,\nu}(it) + G_{\beta,\nu+1+\beta}(it)$$

$$= (\nu+1)(it)\vartheta - \frac{\hat g_1(1)}{t^{\nu+2+\beta}}.$$

Here, we used (3.21) and thus arrive at

$$\operatorname{sign}\operatorname{Re}\frac{d\lambda}{d\vartheta} = -\operatorname{sign}\operatorname{Re}\hat g_1(1)\,. \tag{3.24}$$

We require this quantity is nonzero, which is equivalent to transversal eigenvalue crossing.

We proceed to compute. Expanding $\gamma = \gamma_0 + \varepsilon\gamma_1 + \varepsilon^2\gamma_2 + \dots$ we find $\gamma_0 = g_0$, $\gamma_1 = \mu_1 g_1$, $\gamma_2 = \mu_2 g_1 + \frac{1}{2}\mu_1^2 g_2$. Plugging into (3.20), at the respective orders ε, ε^2, and ε^3 we find

$$0 = Lv_1 := \delta_0\partial_s v_1 + \gamma_0 * v_1, \tag{3.25}$$

$$0 = Lv_2 + (\delta_1\partial_s + \gamma_1 *)v_1 + v_1\gamma_0 * v_1, \tag{3.26}$$

$$\begin{aligned} 0 = {} & Lv_3 + (\delta_2\partial_s + \gamma_2 *)v_1 + v_2(\gamma_0 * v_1) + v_1(\gamma_0 * v_2) \\ & + (\delta_1\partial_s + \gamma_1 *)v_2 + v_1(\gamma_1 * v_1). \end{aligned} \tag{3.27}$$

By what we have said in subsection 3.2, equation (3.25) should have two-dimensional kernel N_0 spanned by $\cos s$ and $\sin s$ (or $e^{\pm is}$). Due to translation equivariance of the problem, we may suppose that the amplitude and phase of this mode of v are normalized so that $v_1(s) = \cos s$.

Now, in terms of Fourier series $v = \sum_{k\in\mathbb{Z}} \hat v(k)e^{iks}$, an equation $Lv = w$ corresponds to

$$\hat L(k)\hat v(k) = \hat w(k) \quad \text{for all } k \in \mathbb{Z}, \qquad \hat L(k) = ik\delta_0 + \hat g_0(k).$$

This is solvable if and only if the nonresonance condition holds, namely $\hat L(k) \neq 0$ for all k such that $\hat w(k) \neq 0$. Since $\hat L(\pm 1) = 0$ by assuming the first criteria (3.14) for a Hopf transition, we always require $\hat w(\pm 1) = 0$.

Moreover, for the following formal analysis we require the nonresonance condition

$$\hat L(k) = \overline{\hat L(-k)} = ik\delta_0 + \hat g_0(k) \neq 0 \qquad \text{holds for } k = \pm 2. \tag{3.28}$$

Applying these considerations to (3.26), since $L(\cos s) = 0$ we see that the term

$$v_1(\gamma_0 * v_1) = (\cos s)(\delta_0 \sin s) = -\frac{i\delta_0}{4}e^{2is} + c.c.,$$

is nonresonant, provided $\hat L(\pm 2) \neq 0$ as we have assumed. However the terms in δ_1 and μ_1 are resonant. Since $\cos s = \frac{1}{2}e^{is} + c.c.$ we find these terms yield $(i\delta_1 + \mu_1\hat g_1(1))\frac{1}{2}e^{is} + c.c.$ Since we presume $\operatorname{Re}\hat g_1(1) \neq 0$ from (3.15), solvability of (3.26) requires $\mu_1 = 0$, and also $\delta_1 = 0$. The solution for v_2 is

$$v_2(s) = \hat v_2(2)e^{2is} + c.c., \qquad \hat v_2(2) = \frac{i\delta_0}{4}\frac{1}{2i\delta_0 + \hat g_0(2)}. \tag{3.29}$$

Next, we consider the solvability of (3.27). The terms involving δ_1 and γ_1 vanish. It remains to show that the resonant terms are removed by a particular choice of δ_2 and μ_2. For this purpose, noting $\hat g_0(1) = -i\delta_0$ we observe

$$\gamma_0 * v_1 = \hat g_0(1)\hat v_1(1)e^{is} + c.c. = -\frac{i\delta_0}{2}e^{is} + c.c., \qquad \gamma_0 * v_2 = \hat g_0(2)\hat v_2(2)e^{2is} + c.c.,$$

therefore the resonant terms on the right hand side of (3.27) are

$$e^{is}\Big((\delta_2 i+\mu_2\hat g_1(1))\hat v_1(1)+\hat v_2(2)\overline{\hat g_0(1)\hat v_1(1)}+\overline{\hat v_1(1)}\hat g_0(2)\hat v_2(2)\Big)+c.c.$$

$$=\ \frac{1}{2}e^{is}\left(\delta_2 i+\mu_2\hat g_1(1)+(i\delta_0+\hat g_0(2))\hat v_2(2)\right)+c.c.,$$

Since $i\delta_0+\hat g_0(2)=\hat L(2)-i\delta_0$, the resonant terms vanish if μ_2 and δ_2 are given by

$$\mu_2\,\mathrm{Re}\,\hat g_1(1)=-\,\mathrm{Re}\left(\frac{i\delta_0}{4}\frac{\hat L(2)-i\delta_0}{\hat L(2)}\right)=\frac{-\delta_0^2}{4|\hat L(2)|^2}\,\mathrm{Re}\,\hat g_0(2), \tag{3.30}$$

$$\delta_2+\mu_2\,\mathrm{Im}\,\hat g_1(1)=-\,\mathrm{Im}\left(\frac{i\delta_0}{4}\frac{\hat L(2)-i\delta_0}{\hat L(2)}\right)=-\frac{\delta_0}{4}+\frac{\delta_0^2}{4|\hat L(2)|^2}(2\delta_0+\mathrm{Im}\,\hat g_0(2)). \tag{3.31}$$

4. Ranges of parameters yielding bifurcation. In this section we provide some numerical and analytical information regarding the occurrence and direction of Hopf bifurcations as one varies the removal factor η in the limit model (3.2)–(3.4), for a variety of cases involving the exponents $\beta=r/(1-\alpha)$ and $\nu=\alpha/(1-\alpha)$ from (3.5). A particularly intriguing finding is that an infinite number of bifurcation points appear when $\nu=\alpha=0$ and $\beta=r$ is an odd integer greater than 1.

4.1. The case $\beta=r=0$, $\nu\geq 0$. We have explicit formulas in this case, since whenever $\mathrm{Re}\,\lambda>-1$, the substitution $(1+\lambda)y=s$ and a contour deformation argument shows

$$G_{0,\nu}(\lambda)=\frac{\Gamma(\nu+1)}{(1+\lambda)^{\nu+1}}.$$

This case corresponds to removal of clusters in (1.10) at rate independent of size, since $r=0$. When ν is an integer, equation (3.7) can be reduced to an ODE of some order by repeated differentiation. We comment on the connection to similar models in the literature in the Appendix A.

In the present case, we can rigorously describe all eigenvalue crossings and prove transversality.

PROPOSITION. *In case $\beta=0$ and $\nu\geq 0$, an eigenvalue $\lambda=it$ with $t>0$ occurs for some $\eta>0$ if and only if*

$$\tan^{-1}t=\omega_k:=\frac{\pi}{2}\frac{1+4k}{1+\nu}\quad \textit{for some integer } k \textit{ satisfying } 0\leq 4k<\nu.$$

The transversal crossing condition (3.15) holds for all k, with $\mathrm{sign}\,\mathrm{Re}\,\frac{d\lambda}{d\vartheta}<0$.

The reason this is true is that the condition (3.14) for eigenvalue crossings takes the form

$$-\arg G_{0,\nu}(it)=(\nu+1)\arg(1+it)=(\nu+1)\tan^{-1}t=\frac{\pi}{2}\ (\mathrm{mod}\,2\pi),$$

and transversality follows from (3.13). We note that large η (or ϑ) corresponds to small t, so that as η decreases from large values (where one has linear stability), a first crossing appears at

$$t_0=\tan\omega_0,\qquad \eta_0=\frac{\vartheta_0}{\Gamma(\nu+1)}=\frac{\cos^{\nu+2}\omega_0}{\sin\omega_0},\qquad \kappa_0=\cos^{\nu+1}\omega_0. \tag{4.1}$$

In summary, for $\beta=0$ we find that whenever $\nu>0$, bifurcation from a stable state should occur at wave number κ_0 as η decreases through the value in (4.1). However, no bifurcation occurs for $\nu=0$. The values of η_2 and κ_2 are in principle explicitly computable, but the expressions become quickly impractical.

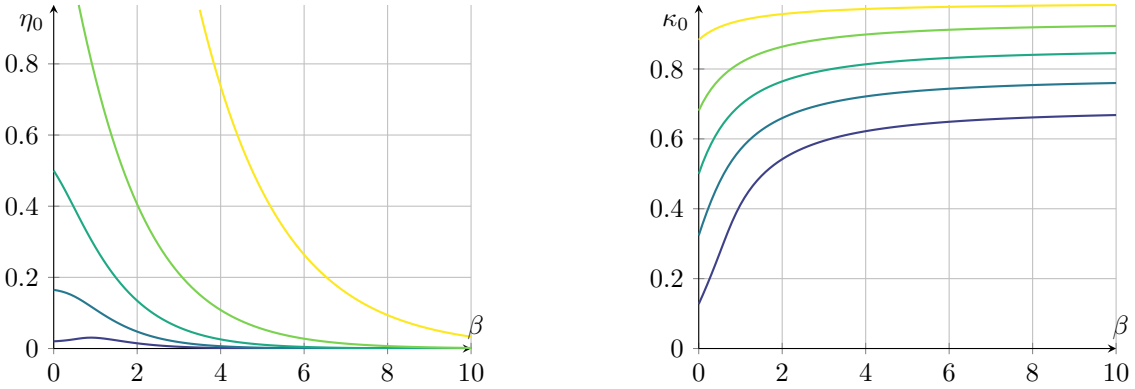

Fig. 3: η_0 (left) and κ_0 (right) vs β for $\nu = \frac{1}{9}$ (——), $\frac{3}{7}$ (——), 1 (——), $\frac{7}{3}$ (——), and 9 (——).

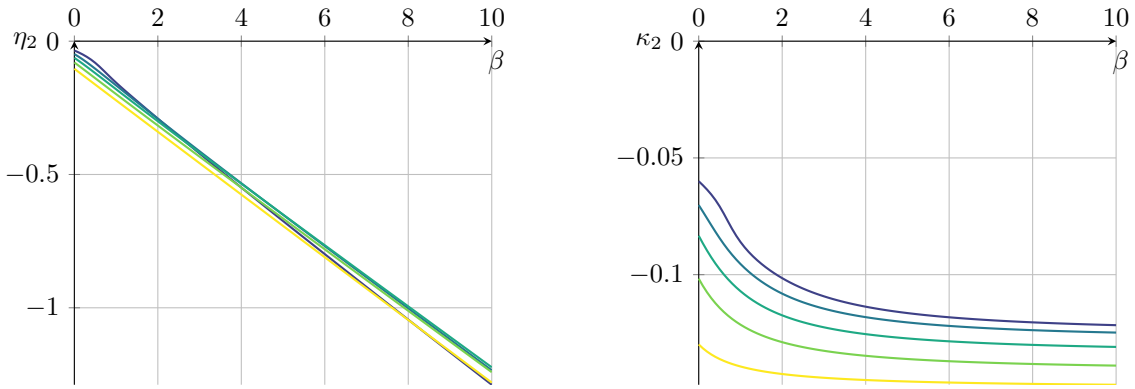

Fig. 4: η_2 (left) and κ_2 (right) vs β for $\nu = \frac{1}{9}$ (——), $\frac{3}{7}$ (——), 1 (——), $\frac{7}{3}$ (——), and 9 (——).

4.2. Numerical bifurcation curves. In Figure 3, we plot the largest value of η_0 corresponding to a solution of the bifurcation criteria (3.14) against the parameter β for various values of ν. The transversality condition (3.15) and nonresonance condition (3.28) are verified numerically in the supplementary material SM2 (see Table SM1 and Table SM2). In Figure 4, we plot values of η_2 and κ_2 from (3.23) to numerically determine the direction of bifurcation. The fact that $\eta_2 < 0$ indicates that $\eta < \eta_0$ along the bifurcating branch, so we expect a supercritical Hopf bifurcation with stable periodic solutions. The values of κ_2 are also negative, which shows that wavenumber decreases as amplitude increases along the branch.

4.3. The case $\beta = r > 0, \nu = 0$. First, we claim that no bifurcation occurs for any $\eta > 0$ if $\nu = 0$ and $\beta = r \in (0, 1]$. Note

$$H_{\beta,0}(t) := \operatorname{Re} G_{\beta,0}(it) = \frac{1}{2}\int_{-\infty}^{\infty} \exp\left(-\frac{|y|^{\beta+1}}{\beta+1} - ity\right) dy\,.$$

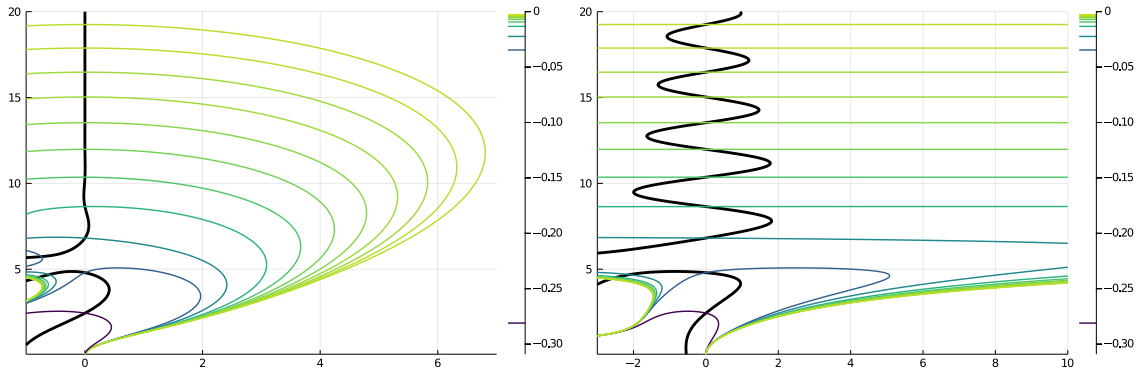

Fig. 5: Contours of $\operatorname{Im} G(\lambda)/\lambda = 0$ (black) and $\operatorname{Re} G(\lambda)/\lambda = -\vartheta_0$ for values ϑ_0 given in Table 1 (blue to lemon). (Left: unscaled. Right: real axis expanded to compensate the exponential factor in (4.2))

For $\beta = 1$ this is a Gaussian and it never vanishes. For $0 < \beta < 1$, the function $h_\beta(y) = \exp(-|y|^{\beta+1}/(\beta+1))$ is the characteristic function (Fourier transform) of a symmetric α-stable distribution from probability theory, with $\alpha = \beta + 1$, see [15, Sec. XVII.6]. Hence $H_{\beta,0}(t)$ is a positive multiple of this distribution's density, which can have no zeros due to its scaling invariance under convolution. Hence (3.14) cannot hold.

For $\beta > 1$, the inverse Fourier transform of h_β is known *not* to be a probability density, and this means $H_{\beta,0}(t)$ *must* cross zero for some t. Transverse crossings would then ensure bifurcation, since $\operatorname{Im} G_{\beta,0}(it) = -\int_0^\infty h_\beta(y)\sin(y)\,dy < 0$ due to the monotonic decrease of h_β.

Odd $\beta > 1$. Strikingly, asymptotics suggests that *infinitely many* bifurcations occur for odd integers $\beta > 1$ in particular. For in this case, h_β is an entire function, and its Fourier transform $H_{\beta,0}(t) \to 0$ as $|t| \to \infty$ at a super-exponential rate. A standard saddle-point analysis (details omitted) indicates

$$H_{\beta,0}(t) \sim \sqrt{\frac{2\pi}{\beta}}\, t^{\frac{1-\beta}{2\beta}} \exp\left(t^{\frac{\beta+1}{\beta}} c_\beta\right) \cos\left(t^{\frac{\beta+1}{\beta}} s_\beta - \frac{\pi}{4}\frac{\beta-1}{\beta}\right) \qquad \text{as } t \to \infty, \tag{4.2}$$

$$\text{where} \qquad c_\beta = \frac{\beta}{\beta+1}\cos\frac{\pi}{2}\frac{\beta+1}{\beta} < 0, \qquad s_\beta = \frac{\beta}{\beta+1}\sin\frac{\pi}{2}\frac{\beta+1}{\beta} > 0.$$

Furthermore $G_{\beta,0}(it) \sim 1/it$ as $t \to \infty$ (integrate (3.10) by parts). Hence, at the bifurcation points that approximate the zeros of (4.2), the bifurcation parameter η and wave number in (3.16) satisfy

$$\vartheta = \eta^{\frac{1}{\beta+1}} G_{\beta,0}(0) \sim \frac{1}{t^2}, \qquad \kappa \sim \frac{t^{-1}}{G_{\beta,0}(0)}.$$

In Figure 5 we observe that at successive bifurcation points, evidently eigenvalues cross the imaginary axis in opposite directions, according to (3.13). Numerics[1] (see column RelErr in Table 1) indicates that for $\beta = 3$, the approximation in (4.2) is reasonably good already for the first zero, where $\operatorname{Re}\frac{d\lambda}{d\vartheta} < 0$ by (3.24).

[1]The integrals $G(\lambda)$ and roots are computed in Julia [7] using the QuadGK [20] and Roots package.

index	ϑ_0	η_0	κ_0	η_2	κ_2	$\operatorname{Re}\hat{g}_1(1)$	$\lvert\hat{L}(2)\rvert$	RelErr
1	2.810^{-1}	2.310^{-3}	5.353^{-1}	-4.355^{-1}	-1.089^{-1}	7.611^{1}	2.947^{0}	1.461^{-2}
2	3.456^{-2}	5.284^{-7}	1.293^{-1}	-2.702^{-1}	-6.755^{-2}	-7.282^{2}	1.091^{0}	2.729^{-3}
3	2.236^{-2}	9.259^{-8}	1.189^{-1}	-3.414^{-1}	-8.535^{-2}	9.813^{2}	1.576^{0}	1.106^{-3}
4	1.326^{-2}	1.143^{-8}	8.942^{-2}	-3.314^{-1}	-8.284^{-2}	-6.708^{2}	1.482^{0}	5.941^{-4}
5	9.327^{-3}	2.803^{-9}	7.538^{-2}	-3.335^{-1}	-8.339^{-2}	3.240^{2}	1.502^{0}	3.700^{-4}
6	6.962^{-3}	8.700^{-10}	6.507^{-2}	-3.332^{-1}	-8.330^{-2}	-1.266^{2}	1.499^{0}	2.524^{-4}
7	5.459^{-3}	3.288^{-10}	5.763^{-2}	-3.333^{-1}	-8.333^{-2}	4.292^{1}	1.500^{0}	1.831^{-4}
8	4.427^{-3}	1.422^{-10}	5.190^{-2}	-3.333^{-1}	-8.333^{-2}	-1.313^{1}	1.500^{0}	1.388^{-4}
9	3.683^{-3}	6.818^{-11}	4.735^{-2}	-3.333^{-1}	-8.333^{-2}	3.718^{0}	1.500^{0}	1.089^{-4}
10	3.127^{-3}	3.542^{-11}	4.362^{-2}	-3.333^{-1}	-8.333^{-2}	-9.911^{-1}	1.500^{0}	8.766^{-5}
11	2.698^{-3}	1.962^{-11}	4.052^{-2}	-3.333^{-1}	-8.333^{-2}	2.517^{-1}	1.500^{0}	7.209^{-5}

Table 1: Numerical values of the first 11 roots of $H_{3,0}(t)$, the transversal crossing condition (3.24), the nonresonance condition (3.28) and relative error to approximate solution from (4.2).

Thus as η decreases through the largest bifurcation point, one pair of eigenvalues emerges into the right half plane and the stable constant state becomes unstable. Decreasing across the next bifurcation point, some pair of eigenvalues must cross back into the left half plane, and it must be the same pair. So the constant state alternates stability between successive bifurcation points.

For small η the instabilities are extremely weak, however. The unstable eigenvalue becomes super-exponentially close to the imaginary axis since $|G'(\lambda)|$ decays only algebraically. Thus for small η the constant state becomes essentially neutrally stable.

Since Table 1 indicates $\eta_2 < 0$ in (3.23) in every case, our study of the direction of bifurcation in section 3.3 indicates that a branch of periodic solutions emerges for η *below* each bifurcation point η_0. We expect that the emerging periodic solutions alternate between stable and unstable, corresponding to the stability of the constant flux solution just *above* η_0.

Regarding what may happen to bifurcating solutions in the large we have no firm information. One relatively simple possibility is that, as η decreases, each bifurcating branch reconnects with the next branch, but only after folding over at some lower value of η and changing its stability.

Other $\beta > 0$ not odd. It is possible to show that some eigenvalue crossing must always occur when $\beta \in (4k+1, 4k+3)$ for some $k \in \mathbb{N}_0$. For in this case we can study the asymptotics of large roots of equation (3.11), and show the constant flux solution becomes unstable as $\eta \to 0$. From Section 3.1 we know it is stable for large η, so some eigenvalue must cross the imaginary axis.

We approximate $G(\lambda) = G_{\beta,0}(\lambda)$ as $|\lambda| \to \infty$ with $\operatorname{Re}(\lambda) \geq 0$ by integrating by parts to get

$$G(\lambda) = \frac{1}{\lambda} - \frac{1}{\lambda}\int_0^\infty \exp\left(-\frac{y^{\beta+1}}{\beta+1}\right) e^{-\lambda y} y^\beta \, dy = \frac{1}{\lambda} + O\left(\frac{1}{|\lambda|^{2+\beta}}\right). \tag{4.3}$$

Thanks to the first exponential factor in the integrand, this expansion is valid for any $\beta \geq 0$ in the region $\operatorname{Re}(\lambda) \geq -1 + \delta$ for any $\delta > 0$. We obtain the leading order approximation

$$\vartheta\lambda + \frac{1}{\lambda} = 0, \qquad \text{hence} \qquad \lambda \simeq \pm\frac{i}{\sqrt{\vartheta}} \qquad \text{as} \quad \vartheta \to 0\,. \tag{4.4}$$

In order to check the stability of these roots, we need to compute the next order of $G(\lambda)$ in (4.3). By a change of variables $z = \lambda y$ and using a contour deformation for large values of z to keep the contour in the region with $\mathrm{Re}(z) \geq 0$, we get

$$\begin{aligned}\int_0^\infty \exp\Big(-\frac{y^{\beta+1}}{\beta+1}\Big) e^{-\lambda y} y^\beta dy &= \frac{1}{\lambda^{1+\beta}} \int_{\frac{\lambda}{|\lambda|}\mathbb{R}} \exp\Big(-\frac{z^{\beta+1}}{(\beta+1)\lambda^{1+\beta}}\Big) e^{-z} z^\beta dz \\ &\simeq \frac{1}{\lambda^{1+\beta}} \int_0^\infty e^{-z} z^\beta dz = \frac{\Gamma(\beta+1)}{\lambda^{1+\beta}} \qquad \text{as } |\lambda| \to \infty\,.\end{aligned}$$

This is valid for any $\beta \geq 0$ in the region $\mathrm{Re}(\lambda) \geq -1+\delta$ for $\delta > 0$. Hence from (4.3), we get the asymptotics $G(\lambda) \simeq \lambda^{-1} - \Gamma(\beta+1)\lambda^{-(\beta+2)}$ for $|\lambda| \gg 1$. Here, the branch of the analytic function is chosen by extending analytically such that $1^{2+\beta} = 1$. We then approximate equation (3.11) as

$$\vartheta\lambda^2 + 1 - \frac{\Gamma(\beta+1)}{\lambda^{1+\beta}} \simeq 0\,. \tag{4.5}$$

We consider the approximation of the root with positive imaginary part in (4.4). By dividing (4.5) by ϑ and taking the square root, we get

$$\lambda = \frac{i}{\sqrt{\vartheta}} \left(1 + \frac{\Gamma(\beta+1)}{\lambda^{1+\beta}}\right)^{\frac{1}{2}} \simeq \frac{i}{\sqrt{\vartheta}} \left(1 - \frac{\Gamma(\beta+1)}{2\lambda^{1+\beta}}\right) \qquad \text{for } |\lambda| \gg 1\,.$$

With the leading approximation of λ from (4.4), we obtain

$$\lambda \simeq \frac{i}{\sqrt{\vartheta}} \left(1 - \frac{\Gamma(\beta+1)\,\vartheta^{\frac{1+\beta}{2}}}{2} \exp\Big(-\frac{i\pi(\beta+1)}{2}\Big)\right) \qquad \text{as} \quad \vartheta \to 0\,, \tag{4.6}$$

where we used $i^{1+\beta} = e^{\frac{i\pi(\beta+1)}{2}}$. For $\beta = 0$, we obtain $\mathrm{Re}(\lambda) \simeq -\frac{1}{2}$, consistent with the result from Section 4.1 that the constant flux state is linearly stable. Regarding the general case, we find

$$\mathrm{sign}\big(\mathrm{Re}(\lambda)\big) \simeq -\,\mathrm{sign}\left(\sin\left(\frac{\pi(\beta+1)}{2}\right)\right) \qquad \text{as } \vartheta \to 0\,. \tag{4.7}$$

Thus we obtain linear instability for $\beta \in (4k+1, 4k+3)$ with $k \in \mathbb{N}_0$, as mentioned above. In case $\beta \in (4k-1, 4k+1)$ for $k \in \mathbb{N}_0$, we have $\mathrm{Re}(\lambda) < 0$ for a root of (3.11) satisfying (4.6), but we do not know about other roots. Nevertheless, this analysis suggests that in the limit $\vartheta \to 0$, the constant flux state changes its stability as β passes an odd integer, which is exactly when the system shows infinitely many bifurcations as discussed in Section 4.3.

The case $\beta \geq 0$ not odd and $\nu \ll 1$. We close this section by indicating that an analysis is possible for the case $\beta \geq 0$ not odd with $\nu \ll 1$ but positive. In the supplementary material SM3, we arrive, consistent with (4.4), at the approximation of the root λ of (3.11) with positive imaginary real part to second order as

$$\lambda \simeq \left(\frac{\Gamma(\nu+1)}{\vartheta}\right)^{\frac{1}{\nu+2}} (i + \lambda_2) \qquad \text{as} \quad \vartheta \to 0,$$

with $\lambda_2 = O(\vartheta^{\frac{\beta+1}{\nu+2}})$. The real part of λ_2 determines the stability of the stationary solution. Approximating λ_2 in the limit $\nu \to 0$, we find

$$\mathrm{Re}(\lambda_2) \simeq \frac{\pi\nu}{4} - \frac{\Gamma(\beta+1)}{2}\vartheta^{\frac{\beta+1}{\nu+2}} \sin\Big(\frac{\pi(\beta+1)}{2}\Big) \qquad \text{as} \quad \nu \to 0. \tag{4.8}$$

First, for $\nu = 0$, we recover the stability condition (4.7). Next, for $\nu > 0$, the stationary solution becomes unstable as soon as ϑ is small enough and oscillatory behavior can be expected, in accordance to the asymptotics from Section 3.3. Finally, we obtain a curve of stability with ν depending on ϑ if $\sin\big(\frac{\pi(\beta+1)}{2}\big) > 0$, that is $\beta \in (4k-1, 4k+1)$ for some $k \in \mathbb{N}_0$.

Appendix A. Moment models. In [17, p. 293ff] a model is suggested for the distribution of diameter sizes of supercritical particles in the presence of homogeneous and heterogeneous nucleation having similarities to the limit model in Section 1.3. Homogeneous nucleation is modeled using an Arrhenius law, and specific power laws for the particle growth and the particle removal are assumed. In [17, (10.46)] constant growth of this diameter is assumed, which translates for our coefficients (1.8) to the case $\alpha = 2/3$. Part of the analysis of this case can also be found in [31].

For this choice of the coefficients, the limit model (1.12)–(1.14) becomes

$$\partial_t f(x,t) + \partial_x\big(x^{\frac{2}{3}} f(x,t)\big) = -\eta x^r f(x,t)\,, \tag{A.1}$$

$$x^{\frac{2}{3}} f(x,t) \simeq e^u \quad \text{as} \quad x \to 0^+\,. \tag{A.2}$$

Following [31], the authors use three moments, denoted as N, A, R which are the number of clusters, the area and the radius, respectively. In our notation these moments are

$$N = \int_0^\infty f(x,t)dx\,, \quad A = \int_0^\infty x^{\frac{2}{3}} f(x,t)dx\,, \quad R = \int_0^\infty x^{\frac{1}{3}} f(x,t)dx\,.$$

It is then possible to calculate the evolution equations for these moments, which we have to complement with the equation for the monomer concentration

$$\partial_t u = 1 - \int_0^\infty x^{\frac{2}{3}} f(x,t)dx = 1 - A.$$

In order to obtain a closed system of ODEs we need to make the removal term precise. In [17], it is assumed that $\eta = 0$, which gives the following system for the moments:

$$\partial_t N = e^u\,, \qquad \partial_t A = \frac{2}{3}R\,, \qquad \partial_t R = \frac{1}{3}N\,, \qquad \partial_t u = 1 - A.$$

This is a system which is not able to generate oscillations, since the moments just grow in time.

In [31] a removal mechanism is suggested that eliminates clusters with a mean life time $\tau > 0$, which is equivalent to choosing $r = 0$ and $\eta = \frac{1}{\tau} > 0$ in (A.1). With this choice, the ODEs for the moments take the form

$$\partial_t N = e^u - \eta N\,, \qquad \partial_t A = \frac{2}{3}R - \eta A\,, \qquad \partial_t R = \frac{1}{3}N - \eta R\,, \qquad \partial_t u = 1 - A\,.$$

This ODE system derived from (A.1) and (A.2) is almost the same as the system considered in [31] with only two minor differences: First, in [31] there is a term associated to the flux of area and

radius at the critical radius present. In our model a similar term is shown to be negligible in the limit that we consider (see (2.20)). Second, for the flux of clusters, as denoted in [17] by I, the full Arrhenius formula is used, whereas we obtain the exponential approximation (2.13) leading to the boundary condition (A.2).

REFERENCES

[1] E. H. M. Badger and I. G. C. Dryden, *The formation of gum particles in coal-gas*, Transactions of the Faraday Society, 35 (1939), p. 607, https://doi.org/10.1039/tf9393500607.

[2] J. M. Ball, J. Carr, and O. Penrose, *The Becker-Döring cluster equations: basic properties and asymptotic behaviour of solutions*, Comm. Math. Phys., 104 (1986), pp. 657–692, http://projecteuclid.org/euclid.cmp/1104115173.

[3] R. C. Ball, C. Connaughton, P. P. Jones, R. Rajesh, and O. Zaboronski, *Collective oscillations in irreversible coagulation driven by monomer inputs and large-cluster outputs*, Phys. Rev. Lett., 109 (2012), p. 168304, https://doi.org/10.1103/physrevlett.109.168304.

[4] K. Bar-Eli and R. M. Noyes, *Gas-evolution oscillators. 10. a model based on a delay equation*, J. Phys. Chem., 96 (1992), pp. 7664–7670, https://doi.org/10.1021/j100198a034.

[5] R. Becker and W. Döring, *Kinetische Behandlung der Keimbildung in übersättigten Dämpfen.*, Ann. der Physik, 24 (1935), pp. 719–752, https://doi.org/10.1002/andp.19354160806.

[6] B. P. Belousov, *A periodic acting reaction and its mechanism*, in Collection of Short Papers on Radiation Medicine, Moscow: Medgiz, 1959, pp. 145–152.

[7] J. Bezanson, A. Edelman, S. Karpinski, and V. B. Shah, *Julia: A fresh approach to numerical computing*, SIAM Review, 59 (2017), pp. 65–98, https://doi.org/10.1137/141000671.

[8] P. G. Bowers and R. M. Noyes, *Chemical oscillations and instabilities. 51. Gas evolution oscillators. 1. Some new experimental examples*, Journal of the American Chemical Society, 105 (1983), pp. 2572–2574, https://doi.org/10.1021/ja00347a010.

[9] N. V. Brilliantov, W. Otieno, S. A. Matveev, A. P. Smirnov, E. E. Tyrtyshnikov, and P. L. Krapivsky, *Steady oscillations in aggregation-fragmentation processes*, Physical Review E, 98 (2018), p. 012109, https://doi.org/10.1103/physreve.98.012109.

[10] S. S. Budzinskiy, S. A. Matveev, and P. L. Krapivsky, *Hopf bifurcation in addition-shattering kinetics*, Phys. Rev. E, 103 (2021), p. L040101, https://doi.org/10.1103/PhysRevE.103.L040101, https://link.aps.org/doi/10.1103/PhysRevE.103.L040101.

[11] J. Carr, D. B. Duncan, and C. H. Walshaw, *Numerical approximation of a metastable system*, IMA J. Numer. Anal., 15 (1995), pp. 505–521, https://doi.org/10.1093/imanum/15.4.505, https://doi.org/10.1093/imanum/15.4.505.

[12] O. Diekmann, S. A. van Gils, S. M. Verduyn Lunel, and H.-O. Walther, *Delay equations*, vol. 110 of Applied Mathematical Sciences, Springer-Verlag, New York, 1995, https://doi.org/10.1007/978-1-4612-4206-2, https://doi.org/10.1007/978-1-4612-4206-2. Functional, complex, and nonlinear analysis.

[13] M. Doumic, K. Fellner, M. Mezache, and H. Rezaei, *A bi-monomeric, nonlinear Becker–Döring-type system to capture oscillatory aggregation kinetics in prion dynamics*, Journal of Theoretical Biology, 480 (2019), pp. 241–261, https://doi.org/10.1016/j.jtbi.2019.08.007.

[14] Y. Farjoun and J. C. Neu, *Exhaustion of nucleation in a closed system*, Physical Review E, 78 (2008), https://doi.org/10.1103/physreve.78.051402.

[15] W. Feller, *An Introduction to Probability Theory and its Applications. Vol. I*, Third edition, John Wiley & Sons Inc., New York, 1968.

[16] R. J. Field and R. M. Noyes, *Oscillations in chemical systems. IV. Limit cycle behavior in a model of a real chemical reaction*, The Journal of Chemical Physics, 60 (1974), pp. 1877–1884, https://doi.org/10.1063/1.1681288.

[17] S. K. Friedlander, *Smoke, Dust, and Haze: Fundamentals of Aerosol Dynamics*, Topics in chemical engineering, Oxford University Press, 2000, https://books.google.de/books?id=fNIeNvd3Ch0C.

[18] J. K. Hale and S. M. Verduyn Lunel, *Introduction to functional-differential equations*, vol. 99 of Applied Mathematical Sciences, Springer-Verlag, New York, 1993, https://doi.org/10.1007/978-1-4612-4342-7, https://doi.org/10.1007/978-1-4612-4342-7.

[19] E. Hingant and R. Yvinec, *Deterministic and Stochastic Becker–Döring Equations: Past and Recent Mathematical Developments*, in Stochastic Processes, Multiscale Modeling, and Numerical Methods for

Computational Cellular Biology, D. Holcman, ed., Springer International Publishing, 2017, pp. 175–204, https://doi.org/10.1007/978-3-319-62627-7_9.

[20] S. G. Johnson, *QuadGK.jl: Gauss–Kronrod integration in Julia*. https://github.com/JuliaMath/QuadGK.jl.

[21] A. J. Lotka, *Contribution to the Theory of Periodic Reactions*, The Journal of Physical Chemistry, 14 (1910), pp. 271–274, https://doi.org/10.1021/j150111a004.

[22] A. J. Lotka, *Undamped oscillations derived from the law of mass action*, Journal of the American Chemical Society, 42 (1920), pp. 1595–1599, https://doi.org/10.1021/ja01453a010.

[23] S. A. Matveev, P. L. Krapivsky, A. P. Smirnov, E. E. Tyrtyshnikov, and N. V. Brilliantov, *Oscillations in Aggregation-Shattering Processes*, Phys. Rev. Lett., 119 (2017), p. 260601, https://doi.org/10.1103/physrevlett.119.260601.

[24] R. McGraw and J. H. Saunders, *A Condensation Feedback Mechanism for Oscillatory Nucleation and Growth*, Aerosol Science and Technology, 3 (1984), pp. 367–380, https://doi.org/10.1080/02786828408959025.

[25] J. S. Morgan, *XXX.—The periodic evolution of carbon monoxide*, J. Chem. Soc., Trans., 109 (1916), pp. 274–283, https://doi.org/10.1039/ct9160900274.

[26] B. Niethammer, *On the evolution of large clusters in the Becker-Döring model*, J. Nonlinear Sci., 13 (2003), pp. 115–155, https://doi.org/10.1007/s00332-002-0535-8.

[27] R. L. Pego and J. J. L. Velázquez, *Temporal oscillations in Becker-Döring equations with atomization*, Nonlinearity, 33 (2020), pp. 1812–1846, https://doi.org/10.1088/1361-6544/ab6815.

[28] O. Penrose, *Metastable states for the Becker-Döring cluster equations*, Comm. Math. Phys., 124 (1989), pp. 515–541, http://projecteuclid.org/euclid.cmp/1104179294.

[29] O. Penrose, *The Becker-Döring equations at large times and their connection with the LSW theory of coarsening*, J. Statist. Phys., 89 (1997), pp. 305–320, https://doi.org/10.1007/BF02770767. Dedicated to Bernard Jancovici.

[30] O. Penrose, J. Lebowitz, J. Marro, M. Kalos, and J. Tobochnik, *Kinetics of a first-order phase transition: computer simulations and theory*, J. Statist. Phys., 34 (1984), pp. 399–426, https://doi.org/10.1007/BF01018552.

[31] S. E. Pratsinis, S. K. Friedlander, and A. J. Pearlstein, *Aerosol reactor theory: Stability and dynamics of a continuous stirred tank aerosol reactor*, AIChE Journal, 32 (1986), pp. 177–185, https://doi.org/10.1002/aic.690320202.

[32] I. Prigogine and R. Lefever, *Symmetry Breaking Instabilities in Dissipative Systems. II*, The Journal of Chemical Physics, 48 (1968), pp. 1695–1700, https://doi.org/10.1063/1.1668896.

[33] A. Schlichting, *Macroscopic limit of the Becker-Döring equation via gradient flows*, ESAIM Control Optim. Calc. Var., 25 (2019), pp. Art. 22, 36, https://doi.org/10.1051/cocv/2018011.

[34] M. Slemrod, *The Becker-Döring equations*, in Modeling in applied sciences, Model. Simul. Sci. Eng. Technol., Birkhäuser Boston, Boston, MA, 2000, pp. 149–171.

[35] K. W. Smith and R. M. Noyes, *Gas evolution oscillators. 3. A computational model of the Morgan reaction*, J. Phys. Chem., 87 (1983), pp. 1520–1524, https://doi.org/10.1021/j100232a014.

[36] K. W. Smith, R. M. Noyes, and P. G. Bowers, *Chemical oscillations and instabilities. part 52. gas evolution oscillators. 2. a reexamination of formic acid dehydration*, The Journal of Physical Chemistry, 87 (1983), pp. 1514–1519, https://doi.org/10.1021/j100232a013.

[37] J. J. Tyson, *The Belousov-Zhabotinskii Reaction*, Springer Berlin Heidelberg, 1976, https://doi.org/10.1007/978-3-642-93046-1.

[38] V. Volterra, *Variazioni efluttuazioni del numero di individui in specie animali conviventi*, Mem. Accad. Lincei, (1926), pp. 31–113.

[39] Z. Yuan, P. Ruoff, and R. M. Noyes, *Chemical oscillations and instabilities. part 66. gas evolution oscillators. 7. a quantitative modeling test for the morgan reaction*, J. Phys. Chem., 89 (1985), pp. 5726–5732, https://doi.org/10.1021/j100272a031.

[40] A. Zhabotinsky, *Periodic course of the oxidation of malonic acid oxidation in a solution*, Biofizika, (1964), pp. 306–311.